Transition States of Amine-Catalyzed Aldol Reactions Involving Enamine Intermediates: Theoretical Studies of Mechanism, Reactivity, and Stereoselectivity

S. Bahmanyar and K. N. Houk*

Contribution from the Department of Chemistry and Biochemistry, University of California, Los Angeles, California 90095-1569

Received June 7, 2001. Revised Manuscript Received August 29, 2001

Abstract: The mechanisms, transition states, relative rates, and stereochemistries of amine-catalyzed aldol reactions involving enamine intermediates have been explored with density functional theory (B3LYP/6-31G*) and CPCM solvation models. Primary enamine-mediated aldol reactions involve half-chair transition states with hydrogen bonding leading to proton transfer. This leads to charge stabilization and low activation energies as compared to secondary enamine-mediated aldol reactions. Oxetane intermediates can be formed when C−C bond formation occurs without H-transfer in the transition state. The stereoselectivities of reactions of ketone enamines with aldehydes, including the facial stereoselectivity involving chiral aldehydes, were modeled and compared with experimental results. Transition states for the intramolecular aldol reactions leading to the formation of hydrindanone-β-ketol and decalone-β-ketol aldol products showed a preference for the formation of the cis-fused rings, in agreement with experimental results.

Introduction

Nature routinely uses enzymatic aldol reactions for the synthesis of carbohydrates.[1] Reactions may involve zinc enolates (Type II aldolases) or enamine intermediates (Type I aldolases) as the reactive nucleophile.[1] Catalytic antibodies have been discovered as well that employ enamine intermediates for aldol reactions.[2,3] In organic synthesis, metal enolate intermediates are usually used for aldol reactions, and the stereochemistry is controlled with chiral enolates, chiral aldehydes, or chiral auxiliaries.[2] Catalytic asymmetric aldol reactions are still relatively novel tools in the synthetic chemists' arsenal. Although much less employed in synthesis, catalytic aldol reactions involving enamines have been long known.[1−8]

Proline-catalyzed asymmetric intramolecular aldol reactions were discovered in the 1970s,[4,5] but only recently were such reactions generalized to intermolecular reactions, by List, Lerner, and Barbas.[6−8] These reactions, like the asymmetric aldol reactions catalyzed by catalytic antibodies and Type I aldolases, involve enamine intermediates as shown in Scheme 1.

The burgeoning interest in antibody- and proline-catalyzed aldol reactions involving enamines has prompted our theoretical investigation of these reactions using density functional theory with the well-established B3LYP/6-31G* method. We have investigated the mechanisms and stereochemistries of aldol reactions catalyzed by primary and secondary amines involving enamine intermediates. We report the results of this study and discuss the mechanisms and transition states of these processes.

Background

Type I aldolases, such as fructose-1,6-biphosphate aldolase, catalyze the biosynthesis of carbohydrates using enamine intermediates.[1,2] Lerner and Barbas developed several catalytic antibodies, such as 38C2 and 33F12, that are Type I aldolase mimics.[2,3] The enzymes and antibodies catalyze stereoselective aldol reactions via enamine-mediated mechanisms with a variety of aldehydes and ketones (Scheme 2).[2,3] A ketone reacts with a lysine residue in the binding cavity to form an enamine. An aldehyde then reacts with the enamine, forming a new C−C bond. The iminium is hydrolyzed to regenerate the lysine and release the aldol product.

Reymond and co-workers, while studying antibody 72D4 that catalyzes aldol reactions via an enamine intermediate, found

(1) (a) Wong, C.-H.; Whitesides, G. M. *Enzymes in Synthetic Organic Chemistry*; Pergamon: Oxford, 1994 and references therein. (b) Fessner, W.-D.; Walter, C. *Top. Curr. Chem.* **1996**, *184*, 98−183 and references therein.

(2) Machajewski, T. D.; Wong, C.-H. *Angew. Chem., Int. Ed.* **2000**, *39*, 1352−1374 and references therein.

(3) (a) Wagner, J.; Lerner, R. A.; Barbas, C. F., II. *Science* **1995**, *270*, 1797−1800. (b) Barbas, C. F., III; Heine, A.; Zhong, G.; Hoffmann, T.; Gramatikova, S.; Björnestedt, R.; List, B.; Anderson, J.; Stura, E. A.; Wilson, I. A.; Lerner, R. A. *Science* **1997**, *278*, 2085−2092. (c) Hoffmann, T.; Zhong, G.; List, B.; Shabat, D.; Anderson, J.; Gramatikova, S.; Lerner, R. A.; Barbas, C. F., III. *J. Am. Chem. Soc.* **1998**, *120*, 2768−2779. (d) Zhong, G.; Hoffmann, T.; Lerner, R. A.; Danishefsky, S.; Barbas, C. F., III. *J. Am. Chem. Soc.* **1997**, *119*, 8131−8132. (e) List, B.; Lerner, R. A.; Barbas, C. F., III. *Org. Lett.* **1999**, *1*, 1623−1626.

(4) (a) Hajos, Z. G.; Parrish, D. R. Asymmetric Synthesis of Optically Active Polycyclic Organic Compounds. German Patent DE 2102623, Jul 29, 1971. (b) Hajos, Z. G.; Parrish, D. R. *J. Org. Chem.* **1973**, *38*, 3239−3243. (c) Hajos, Z. G.; Parrish, D. R. *J. Org. Chem.* **1974**, *39*, 1615−1621. (d) Hajos, Z. G.; Parrish, D. R. Perhydroin-1,5-diones and 1,6-Tetralindiones. U.S. Patent 3975440, Aug 17, 1976 (Assignee: Hoffmann-La Roche Inc., Nutley, NJ 07110).

(5) (a) Eder, U.; Sauer, G.; Wiechert, R. (Schering A.-G.). Optically active 1,5-Indanone and 1,6-Napthalenedione. German Patent DE 2014757, Oct 7, 1971. (b) Eder, U.; Sauer, G.; Wiechert, R. *Angew. Chem., Int. Ed. Engl.* **1971**, *10*, 496−497.

(6) (a) List, B.; Lerner, R. A.; Barbas, C. F., III. *J. Am. Chem. Soc.* **2000**, *122*, 2395−2396.

(7) (a) Notz, W.; List, B. *J. Am. Chem. Soc.* **2000**, *122*, 7386−7387. (b) List, B.; Pojarliev, P.; Castello, C. *Org. Lett.* **2001**, *3*, 573−575. (c) List, B. Private communication.

(8) Sakthivel, K.; Notz, W.; Bui, T.; Barbas, C. F., III. *J. Am. Chem. Soc.* **2001**, *123*, 5260−5267.

10.1021/ja011403h CCC: $20.00
Published on Web 10/23/2001

Scheme 1. Mechanism of Amine-Catalyzed Aldol Reactions Involving Enamine Intermediates

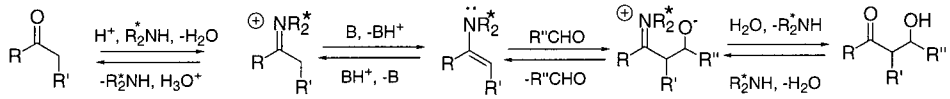

Scheme 2. Examples of Enzyme and Antibody-Catalyzed Reactions

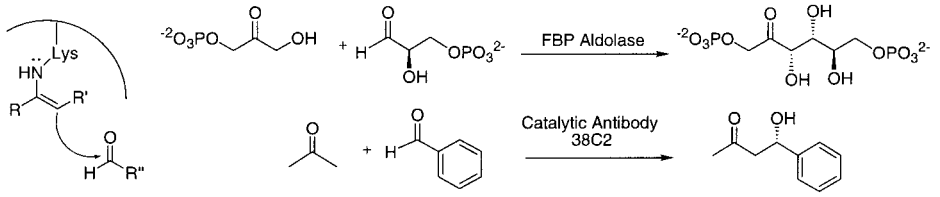

Scheme 3. Intermolecular Aldol Reactions Catalyzed by Amines **1** and **2**

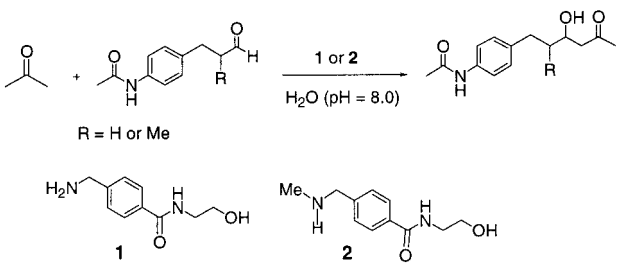

Scheme 4. Aldol Reactions Catalyzed by Primary and Secondary Amines

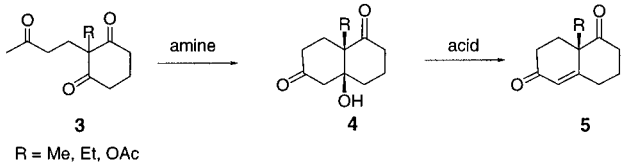

that the intermolecular aldol reactions of acetone with aldehydes can be catalyzed by primary and secondary amines.[9] They also studied a variety of amine-catalyzed aldol reactions in water and reported that primary amines react faster than secondary amines with the exception of the amino acid proline.[9] Primary amine **1** was found to catalyze the stereoselective aldol reaction shown in Scheme 3, 10 times faster than secondary amine **2**.[9] Kinetic studies indicated that the rate-determining step of the enamine-catalyzed aldol reaction is the C−C bond-forming step.[9]

Primary amines such as methylamine, *n*-butylamine, and a variety of amino acids and secondary amines such as pyrrolidine, morpholine, and the amino acid proline have also been used to catalyze intramolecular aldol reactions (Scheme 4).[4,5,9,10] Starting with diketone **3**, where R is methyl, ethyl, or acetate, the cis-fused decalone-β-ketol intermediate **4** is the major product isolated from this intramolecular aldol reaction, which upon dehydration leads to the formation of the α,β-unsaturated cis-fused decalone **5**.

Hajos and Parrish,[4] and independently Eder, Sauer, and Wiechert,[5] reported the first asymmetric proline-catalyzed asymmetric intramolecular aldol reactions (Scheme 5). L-(*S*)-Proline catalyzes the stereoselective formation of the cis-fused (*S*,*S*)-hydrindanone-β-ketol intermediate, **6**,[4] which upon dehydration forms the cis-fused (*S*)-α,β-unsaturated hydrindanone, **7**.[4,5] Other amino acids and amino acid derivatives, such as alanine, phenylalanine, and (*S*)-α-methyl benzylamine, were also used as catalysts for these stereoselective reactions, but the enantioselectivities were lower.[4,5,11] Subsequent studies reported that other derivatives of proline, such as esters and amides, also catalyze the same reactions with lower enantioselectivities.[4,12]

Scheme 5. Proline-Catalyzed Asymmetric Aldol Reactions

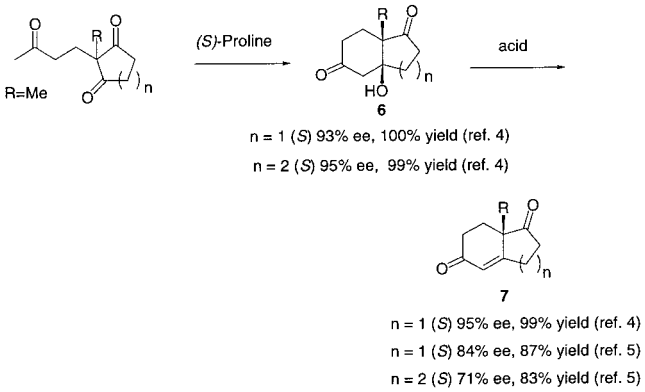

Scheme 6. Proline-Catalyzed Asymmetric Aldol Cyclodehydration Reactions

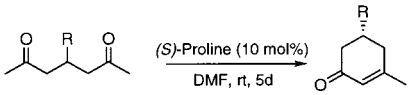

More recently, Agami et al. studied proline-catalyzed cyclodehydration reactions of acyclic derivatives; they also observed moderate enantioselectivities as shown in Scheme 6.[13] In the past two years, Lerner, List, and Barbas reported the first proline-catalyzed asymmetric intermolecular aldol reactions,[6] and these studies have been extended to other substrates (Scheme 7).[7,8]

Aldol and related reactions involving enamine intermediates have been studied theoretically. Sevin et al. studied the aldol reaction of vinylamine and formaldehyde using ab initio (RHF/

(9) (a) Reymond, J. L.; Chen, Y. *J. Org. Chem.* **1995**, *60*, 6970−6979. (b) Reymond, J. L. *J. Mol. Catal. B.: Enzymatic* **1998**, *5*, 331−337 and references therein.

(10) (a) Spencer, T. A.; Neel, H. S.; Flechtner, T. W.; Zayle, R. A. *Tetrahedron Lett.* **1965**, *43*, 3785−3793. (b) Spencer, T. A.; Schmiegel, K. K.; Williamson, K. L. *J. Am. Chem. Soc.* **1963**, *85*, 3785−3793. (c) Danishefsky, S.; Cain, P. *J. Am. Chem. Soc.* **1976**, *98*, 4975−4982. (d) Barbas, C. F., III; Bui, T. *Tetrahedron Lett.* **2000**, *41*, 6951−6954.

(11) The amino acid phenylalanine has been used as the catalyst for aldol condensation reactions in the asymmetric synthesis of estrone (see ref 10c) and in the total synthesis of (−)-ilimaquinone (Bruner, S. D.; Radeke, H. S.; Tallarico, J. A.; Snapper, M. L. *J. Org. Chem.* **1995**, *60*, 1114−1115) with good enantioselectivities.

(12) (a) Hiroi, K.; Yamada, S. I. *Chem. Pharm. Bull.* **1975**, *23*, 1103−1109. (b) Terashima, S.; Satu, S.; Koga, K. *Tetrahedron Lett.* **1979**, *36*, 3469−3472.

(13) (a) Agami, C. *Bull. Soc. Chim. Fr.* **1988**, 499−507. (b) Agami, C.; Levisalles, J.; Sevestre, H. *J. Chem. Soc., Chem. Commun.* **1984**, *7*, 418−420.

Scheme 7. Proline-Catalyzed Asymmetric Intermolecular Reactions

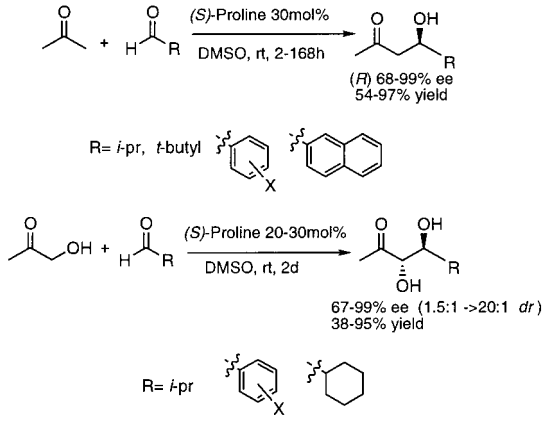

3-21G+CI) methods.[14] They concluded that the concerted transition state corresponding to C−C bond formation accompanied by proton transfer is preferred. They also studied the asymmetric Michael reactions of secondary enamines and enones with ab initio (RHF/6-31G**+CI) and MNDO calculations; chair and boat transition states were found and used to explain stereoselectivities of the reactions of chiral vinyl amines and methyl vinyl ketone.[15] d'Angelo et al. used semiempirical AM1 methods to study the reactions of enamines with methyl acrylate.[16] In our laboratories, Michael reactions of vinyl amines with alkenes were studied with ab initio (HF/6-31G*), semiempirical (PM3), and MM2 force field calculations, and a new model for 1,4-chirality transfer was developed.[17]

Computational Methods

All structures were computed using hybrid density functional theory (B3LYP)[18] and the 6-31G*[19] basis set as implemented in Gaussian 98.[20] Solvation energies were estimated for water ($\epsilon = 78$) using the solvation model CPCM[21] as implemented in Gaussian 98. CPCM is a conductor-like screening solvation model (COSMO) with a continuum polarizable description of solvent that takes into account both electrostatic and van der Waals contributions to calculate gradients and energies. All gas-phase minima and transition structures (referred to here also as transition states) were characterized by frequency analysis. Reported electronic energies include zero point energy corrections scaled by 0.9806.[22] The energies computed for structures in solvent include the electronic energy plus the solvation free energy from CPCM. Charges were computed with the ChelpG method.[23]

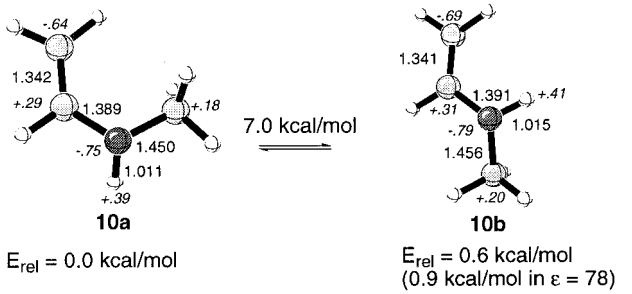

Figure 1. Cis and trans conformens of *N*-methylvinylamine. Partial charges for heavy atoms and NH hydrogens are included.

Scheme 8. Primary Enamine-Mediated Intermolecular Aldol Reaction with and without Proton Transfer

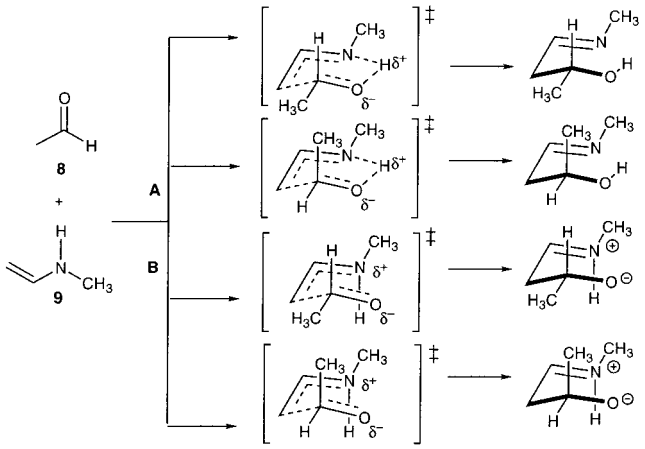

Results and Discussion

Intermolecular Aldol Reactions Involving Primary and Secondary Enamines of Aldehydes. Two mechanisms for the primary enamine-mediated intermolecular aldol reaction of acetaldeyde, **8**, with *N*-methylvinylamine, **9**, were studied (Scheme 8). Mechanism A is a concerted reaction involving both C−C bond formation and proton transfer in a single transition state; this is similar to the well-established ene reaction.[24] Mechanism B involves two transition states; the first step involves C−C bond formation and gives a zwitterionic intermediate, and the second step involves proton transfer.

The s-cis conformation of *N*-methylvinylamine, **10a**, is preferred over the s-trans conformation, **10b**, by 0.6 kcal/mol in the gas phase and by 0.9 kcal/mol in water ($\epsilon = 78$) (Figure 1). This type of conformational preference due to electrostatic effects is also observed in s-cis conformations of enol ethers, amides, and esters.[25] The conformers readily interconvert.

(14) Sevin, A.; Maddaluno, J.; Agami, C. *J. Org. Chem.* **1987**, *52*, 5611−5615.
(15) Sevin, A.; Masure, D.; Geissner-Prettre, C. *Helv. Chim. Acta* **1990**, *73*, 552−573.
(16) Tran Huu Dau, M. E.; Riche, C.; Dumas, F.; d'Angelo, J. *Tetrahedron: Asymmetry* **1998**, *9*, 1059−1064.
(17) (a) Loncharich, R. J.; Houk, K. N. *J. Am. Chem. Soc.* **1987**, *109*, 6947−6953. (b) Thomas, B. E.; Loncharich, R. J.; Houk, K. N. *J. Org. Chem.* **1992**, *57*, 1354−1361. (c) Thomas, B. E.; Houk, K. N. *J. Am. Chem. Soc.* **1993**, *115*, 790, 792. (d) Lucero, M. J.; Houk, K. N. *J. Am. Chem. Soc.* **1997**, *119*, 826−827.
(18) (a) Becke, A. D. *J. Chem. Phys.* **1993**, *98*, 1372−1377. (b) Becke, A. D. *J. Chem. Phys.* **1993**, *98*, 5648−5652. (c) Lee, C.; Yang, W.; Parr, R. G. *Phys. Rev. B* **1988**, *37*, 785−789.
(19) (a) Ditchfield, R.; Hehre, W. J.; Pople, J. A. *J. Chem. Phys.* **1971**, *54*, 724−728. (b) Hehre, W. J.; Ditchfield, R.; Pople, J. A. *J. Chem. Phys.* **1972**, *56*, 2257−2261. (c) Hariharan, P. C.; Pople, J. A. *Theor. Chim. Acta* **1973**, *28*, 213−222.
(20) Frisch, M. J.; Trucks, G. W.; Schlegel, H. B.; Scuseria, G. E.; Robb, M. A.; Cheeseman, J. R.; Zakrzewski, V. G.; Montgomery, J. A., Jr.; Stratmann, R. E.; Burant, J. C.; Dapprich, S.; Millam, J. M.; Daniels, A. D.; Kudin, K. N.; Strain, M. C.; Farkas, O.; Tomasi, J.; Barone, V.; Cossi, M.; Cammi, R.; Mennucci, B.; Pomelli, C.; Adamo, C.; Clifford, S.; Ochterski, J.; Petersson, G. A.; Ayala, P. Y.; Cui, Q.; Morokuma, K.; Malick, D. K.; Rabuck, A. D.; Raghavachari, K.; Foresman, J. B.; Cioslowski, J.; Ortiz, J. V.; Stefanov, B. B.; Liu, G.; Liashenko, A.; Piskorz, P.; Komaromi, I. R.; Gomperts, R.; Martin, L.; Fox, D. J.; Keith, T.; Al-Laham, M. A.; Peng, C. Y.; Nanayakkara, A.; Gonzalez, C.; Challacombe, M. P.; Gill, M. W.; Johnson, B.; Chen, W.; Wong, M. W.; Andres, J. L.; Gonzalez, C.; Head-Gordon, M.; Replogle, E. S.; Pople, J. A. *Gaussian 98*, revision A.6; Gaussian, Inc.: Pittsburgh, PA, 1998.
(21) (a) Barone, V.; Cossi, M. *J. Phys. Chem. A* **1998**, *102*, 1995−2001. (b) Barone, B.; Cossi, M.; Tomasi, J. *J. Comput. Chem.* **1998**, *19*, 404−417.
(22) Scott, A. P.; Radom, L. *J. Phys. Chem.* **1996**, *100*, 16502−16513.
(23) (a) Chirlian, L. E.; Francl, M. M. *J. Comput. Chem.* **1987**, *8*, 894−905. (b) Breneman, C. M.; Wiberg, K. B. *J. Comput. Chem.* **1990**, *11*, 361−373.
(24) (a) Davies, A. G.; Schiesser, C. H. *Tetrahedron* **1991**, *47*, 1707−1726. (b) Chen, J. S.; Houk, K. N.; Foote, C. S. *J. Am. Chem. Soc.* **1997**, *119*, 9852−9855. (c) Singleton, D. A.; Hang, C. *Tetrahedron Lett.* **1999**, *40*, 8939−8943.
(25) Eliel, E. L.; Wilen, S. H.; Mander, L. N *Stereochemistry of Organic Compounds*; John Wiley and Sons: New York, 1994; pp 615−620.

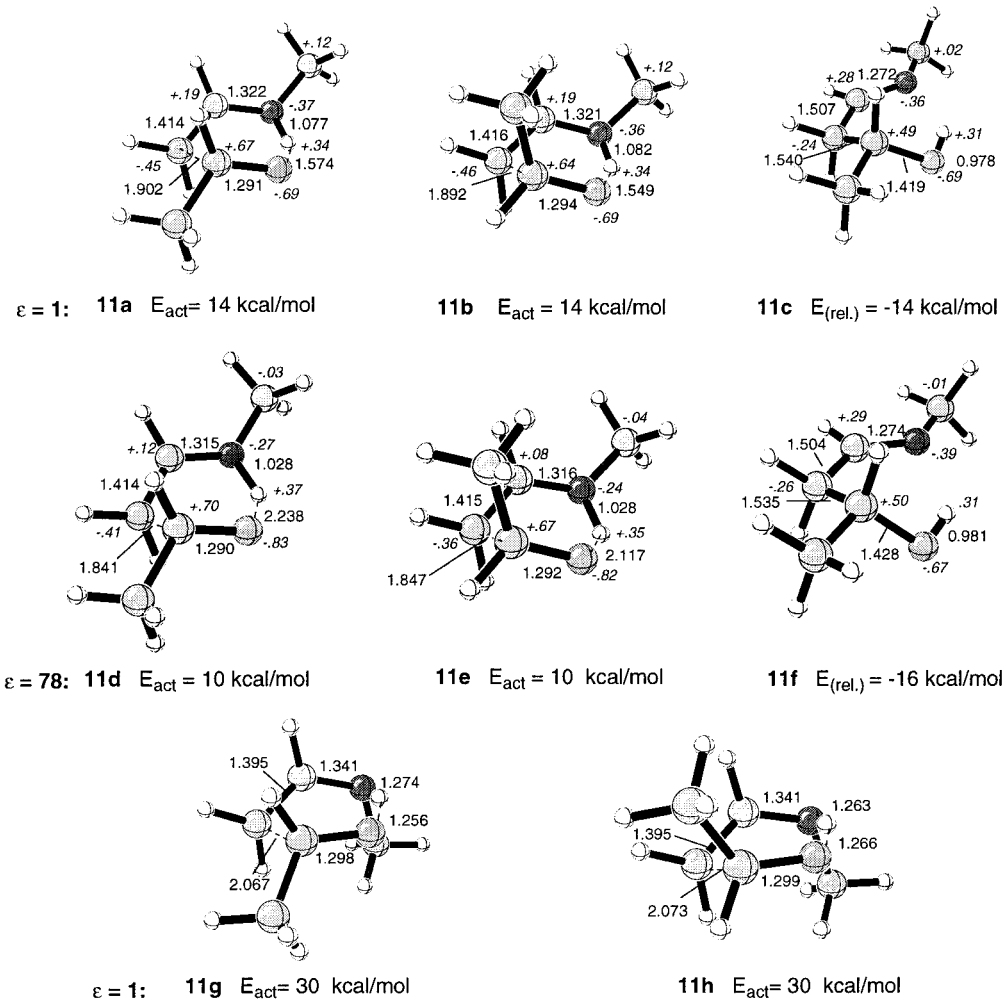

Figure 2. Transition states and products (**11c** and **11f**) for the reaction of *N*-methylvinylamine and acetaldehyde involving concerted C−C bond formation and proton transfer. Partial charges for the heavy atoms and NH hydrogens have been included for structures **11a**−**f**. Energies are relative to reactants.

Transition states were located for the reaction of acetaldehyde, **8**, with *N*-methylvinylamine, **10b** (Figure 2). The transition states, **11a** and **11b**, have a strong hydrogen bond between the NH and the developing alkoxide. Here, the geometry of the transition state is in a half-chair arrangement, where the H is located so as to maintain bonding in the enamine/iminium portion of the transition state and simultaneously hydrogen bond to the developing alkoxide; this hydrogen is transferred as the reaction occurs. There are two possible conformations of the transition state involving an equatorial (**11a**) or axial (**11b)** methyl group. The forming C−C bond length is 1.90 Å, and the C−N bond length is contracted to 1.32 Å in the transition state. The hydrogen on the alkene portion of *N*-methylvinylamine is rotated away from the methyl group of acetaldehyde and does not provide any steric repulsion; consequently, the two stereoisomeric transition states are predicted to be equal in energy. The energy barrier to the reaction is 14 kcal/mol. Intrinsic reaction coordinate (IRC) calculations confirmed the formation of the neutral product **11c** from transition state **11a**. This reaction is predicted to be exothermic by 14 kcal/mol in the gas phase.

These transition states were reoptimized in a water cavity model ($\epsilon = 78$) (Figure 2). The geometries are slightly larger (forming bond 1.84−1.85 Å), and the hydrogen bond is much longer (2.1−2.2 Å in $\epsilon = 78$ instead of 1.5−1.6 Å in $\epsilon = 1$). The energy barrier to reaction is lowered by 4 kcal/mol as compared to that in the gas phase. The partial charges, as indicated in Figure 2, in the transition state are further stabilized by a polar solvent, leading to a lower barrier relative to that in the gas phase. As in the gas phase, **11d** and **11e** are equal in energy in water. The overall reaction is predicted to be exothermic by 16 kcal/mol in $\epsilon = 78$.

Transition states for the reaction of acetaldehyde involving the s-cis conformation **10a** of *N*-methylvinylamine are considerably higher in energy. The transition states, **11g** and **11h**, are held in half-chair conformations by the hydrogen bond between the NH and the developing alkoxide. These transition states are predicted to have a forming C−C bond length of 2.0 Å. The hydrogen bonding in the transition state forces the nitrogen lone-pair out of conjugation with the enamine π-bond and raises the barriers by 16 kcal/mol relative to those of **11a** or **11b**.

The transition states could also be located for reactions not involving H-transfer. Beginning from geometries where the NH is maintained in the enamine plane, transition states with zwitterionic character were located (Figure 3). These transition states, **12a** and **12b**, are much later, with forming C−C bond lengths of 1.66−1.68 Å and C−N bond lengths of 1.31−1.32 Å. Electrostatic interactions, rather than a hydrogen bond, hold the two substrates together (since the NH−O distances are 2.60−2.68 Å). A simple calculation of electrostatic attractions between the H on N ($q = +0.34$ to $+0.36$) with the developing alkoxide ($q = -0.69$ to -0.73) shows that the NH−O hydrogen

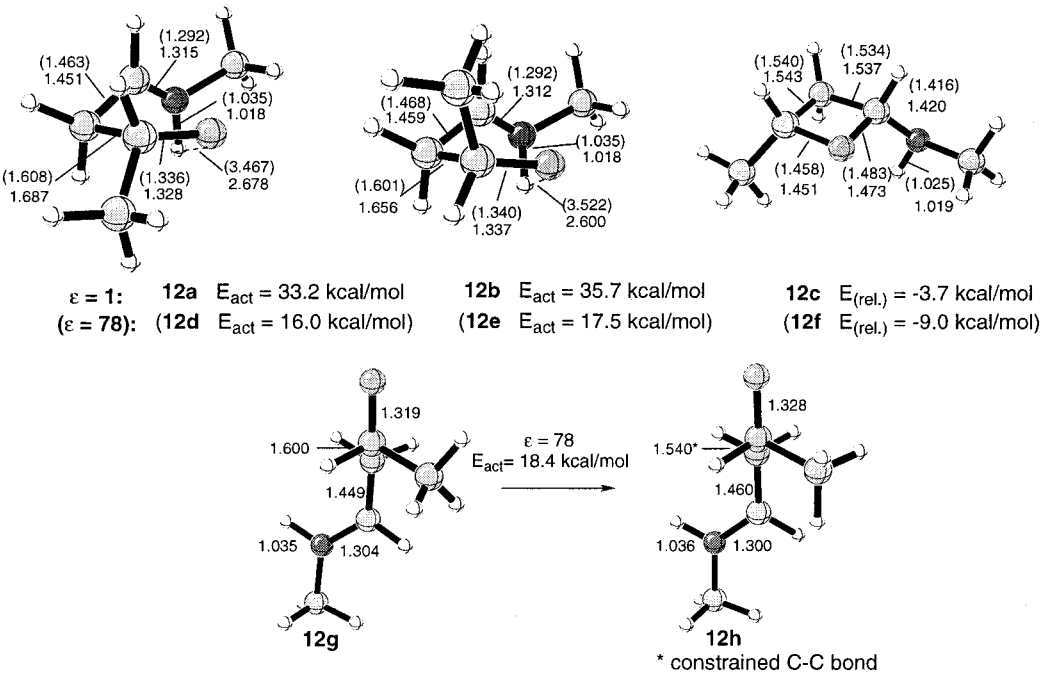

Figure 3. Transition states and products (**12c** and **12f**) for the reaction of *N*-methylvinylamine and acetaldehyde involving zwitterionic processes. Energies are relative to reactants. The "anti" transition state (**12g**) and intermediates (**12h**) for the reaction of *N*-methylvinylamine and acetaldehyde.

Scheme 9. Transition States for the C−C Bond Formation without Proton Transfer Lead to Oxetanes

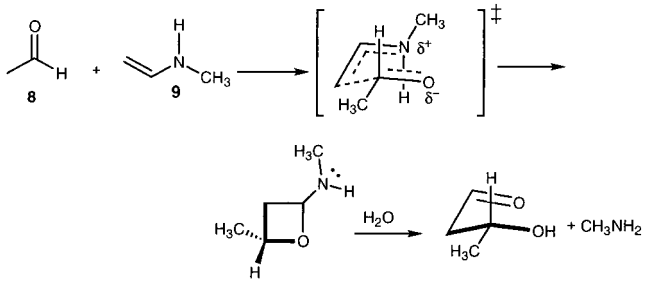

Scheme 10. Secondary Enamine-Mediated Intermolecular Aldol Reactions

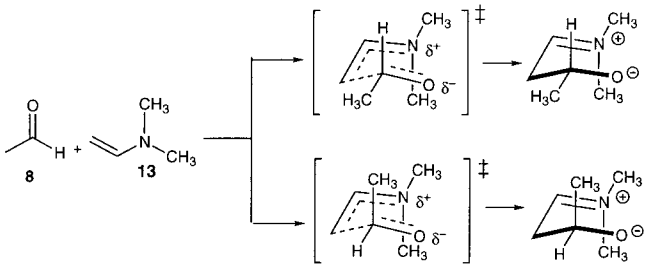

bond can stabilize transition state **11a** by 17 kcal/mol relative to transition state **12a**. The energy barrier to these reactions in the gas phase is predicted to be 33 kcal/mol in the equatorial conformation (**12a**) and 36 kcal/mol in the axial conformation (**12b**). IRC calculations show that these transition states lead to oxetane product, **12c** (Figure 3, Scheme 9), and no stable zwitterion could be located. This reaction is predicted to be only slightly exothermic (−3.7 kcal/mol) in the gas phase.

These transition states were reoptimized in a water cavity model ($\epsilon = 78$) (Figure 3).[26] The hydrogen bond that is so prominent in other transition states is absent in transition states **12d** and **12e** (NH−O = 3.5 Å). The transition states are very late, with forming C−C bond lengths of 1.60 Å and C−N bond lengths of 1.29 Å. The conformer with an axial methyl group (**12e**) is destabilized due to 1,3-diaxial interactions of the acetaldehyde methyl group and hydrogen on the alkene portion of the enamine. The barrier to the reaction is approximately 17 kcal/mol lower in the water dielectric in comparison to that in the gas phase due to stabilization of partial charges in the transition state. In $\epsilon = 78$, once again the product formed was the oxetane ring, **12f**, and the reaction is exothermic by 9.0 kcal/mol. The oxetane ring could be a short-lived intermediate, which upon hydrolysis would give the expected aldol product.

Finally, one transition state, **12g**,[27] was located in $\epsilon = 78$ for the reaction of **10b** with acetaldehyde, where the reactants approach anti relative to one another and there is no possibility of hydrogen bonding, or of good electrostatic stabilization. The barrier to reaction is 18.4 kcal/mol, 2.4 kcal/mol above that of transition state **12d**. Intermediates formed from transition state **12g** could not be located. A geometry optimization involving constraint of the forming C−C bond to 1.54 Å gave a model for a zwitterionic intermediate, **12h**.[28] This model zwitterionic intermediate is only 2 kcal/mol lower in energy than transition state **12g**.

These calculations indicate that, even in water, there is a preference for the transition states with an envelope arrangement of heavy atoms. Electrostatic attraction of charged regions of the zwitterion is favorable, even in polar solvents. The transition states in mechanism A involving hydrogen transfer have lower energy barriers and are highly exothermic. The transition states in mechanism B have no hydrogen bonding and have higher energy barriers.

Secondary enamine-mediated aldol reactions, such as that involving *N*,*N*-dimethylvinylamine, **13** (Scheme 10), can only go to zwitterionic intermediates, since there is no NH or other proton sources to transfer to the developing alkoxide. The transition states, **14a** and **14b**, are shown in Figure 4. Both are late, with forming C−C bond lengths of 1.69 Å and C−N bond lengths of 1.31 Å. The axial conformer **14b** is more destabilized

(26) The energy of transition state **12d** converged to −327.0653 au.
(27) The energy of transition state **12g** converged to −327.0614 au.
(28) The energy intermediate **12h** converged to −327.0643 au.

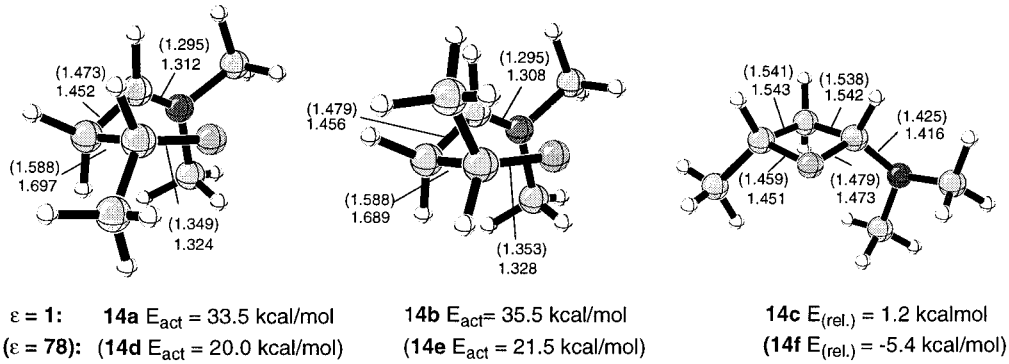

ε = **1:** **14a** E_{act} = 33.5 kcal/mol; **14b** E_{act} = 35.5 kcal/mol; **14c** $E_{(rel.)}$ = 1.2 kcalmol

(ε = **78):** (**14d** E_{act} = 20.0 kcal/mol); (**14e** E_{act} = 21.5 kcal/mol); (**14f** $E_{(rel.)}$ = -5.4 kcal/mol)

Figure 4. Transition states and products (**14c** and **14f**) for the reactions of *N*,*N*-dimethylvinylamine and acetaldehyde involving C−C bond formation. Energies are relative to reactants.

Scheme 11. Secondary Enamine-Mediated Intermolecular Aldol Reactions in the Presence of a Proton Donor

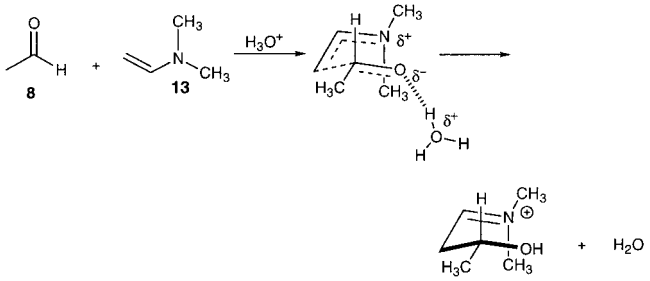

due to the 1,3-diaxial interactions between the methyl group of the acetaldehyde and the hydrogen of the alkene portion of the enamine. These zwitterionic transition states lead to oxetane intermediates (**14c**).

The transition states were reoptimized in a water cavity model ($\epsilon = 78$) (Figure 4).[29] The transition states, **14d** and **14e**, become even later than the gas-phase transition states, and the energy barriers decrease by 14 kcal/mol in water.

To explore how external proton sources or Lewis acids would influence the reaction, we studied the hydronium ion-catalyzed reaction of **8** with **13** (Scheme 11). A detailed analysis of the potential energy surface in the gas phase revealed that this reaction does not have a barrier; the hydronium ion transfers a proton to acetaldehyde and leads directly to the formation of a charged iminium intermediate.

Intramolecular hydrogen bonding in reactions of enamines formed from primary amines plays an important role in stabilizing the developing charges in the transition states of these reactions, reducing the energy barrier of the primary enamine-mediated aldol reactions. Polar solvents also play a key role in lowering energy barriers. The results are consistent with experimental observations made by Reymond et al. that primary amines react faster than secondary amines.[9]

All of these transition states resemble a half-chair six-membered ring with the five heavy atoms in an envelope arrangement. The nucleophilic enamine carbon is out of the plane of the other four heavy atoms. The hydrogen shared by N and O is really in the plane of these four heavy atoms. Consequently, the transition state differs from the familiar chairlike Zimmerman−Traxler[30] transition state drawn for metal enolate and aldol reactions and also found in computational studies of aldol processes.[31] They share in common the staggering about the forming bond and the gauche arrangement of enamine and carbonyl double bonds.

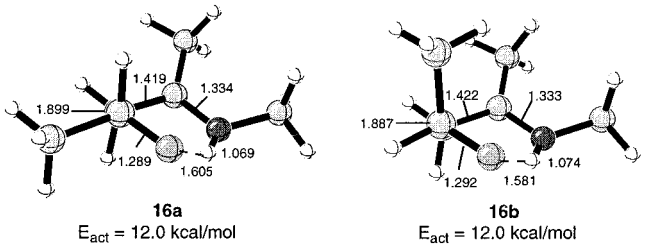

16a E_{act} = 12.0 kcal/mol; **16b** E_{act} = 12.0 kcal/mol

Figure 5. Transition states for reaction of enamine **15** and acetaldehyde.

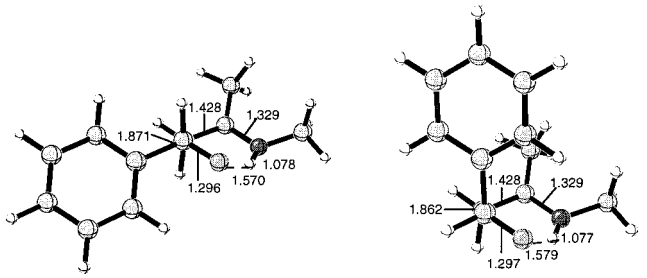

17a E_{rel} = 0.7 kcal/mol; **17b** E_{rel} = 0.0 kcal/mol

Figure 6. Transition states for reaction of enamine **15** and benzaldehyde.

Scheme 12. Reaction of Enamine **15** with Acetaldehyde and Benzaldehyde

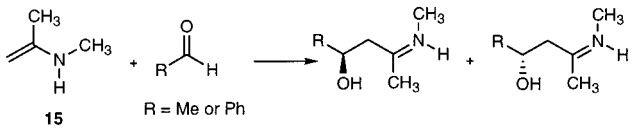

Stereoselectivity of Enamines from Ketones. To determine how ketone enamines differ from aldehyde enamines, transition states **16a** and **16b** for the reaction of enamine **15**, formed from acetone and acetaldehyde, were located (Scheme 12, Figure 5). In the remaining drawings, a Newman projection representation is given to emphasize the staggering about the forming bond that occurs in the half-chair transition state. The transition states have forming C−C bond lengths of 1.89 Å and C−N bond lengths of 1.42 Å. Equatorial (**16a**) and axial (**16b**) transition states have 12.0 kcal/mol energy barriers. The methyl group on the alkene portion of the enamine is rotated back, and potentially destabilizing 1,3-diaxial Me−Me repulsion in the axial transition state is absent.

With benzaldehyde instead of acetaldehyde, the transition states **17a** and **17b**, shown in Figure 6, were obtained. Sur-

(29) The energy of transition state **14e** converged to −366.3665 au.

(30) Zimmerman, H. E.; Traxler, M. D. *J. Am. Chem. Soc.* **1957**, *79*, 1920−1923.

(31) Li, Y.; Paddon-Row, M. N.; Houk, K. N. *J. Org. Chem.* **1990**, *55*, 481−493.

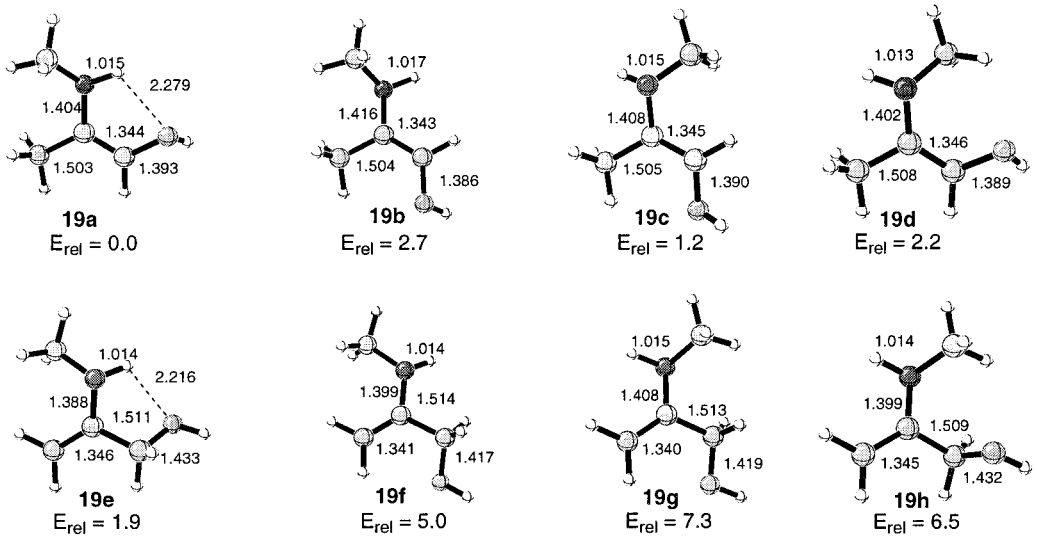

Figure 7. Conformations and isomers of the *N*-methylenamine of hydroxyacetone.

Scheme 13. Reaction of Enamine **18** with Acetaldehyde

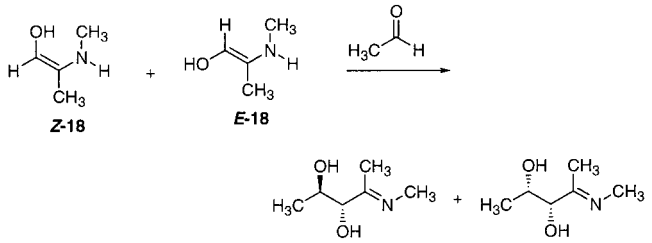

prisingly, the transition state with an axial phenyl substituent (**17b**) is 0.7 kcal/mol lower in energy than that with an equatorial phenyl (**17a**). Stabilizing electrostatic interactions between the partial positive hydrogens of the methyl group of the enamine and the π density of the phenyl ring are believed to result in the lowering of the energy of the axial transition state. This electrostatic attraction is worth 0.6 kcal/mol when estimated with a simple Coulomb's law calculation using the partial charges of the phenyl ring and the hydrogens of the methyl group of transition state **17b**.

Hydroxyacetone, which reacts in enzyme (as a phosphate derivative),[1] antibody,[2,3] and simple amine-catalyzed[9,10] aldol reactions, gives a hydroxyl-substituted enamine intermediate, **18** (Scheme 13). The enzyme- and antibody-catalyzed reactions are reported to be more facile when hydroxyacetone is used instead of acetone.[3c]

We first explored the various conformations and isomers of the *N*-methyl enamine of hydroxyacetone (Figure 7). The intramolecular hydrogen-bonded species are more stable than those lacking hydrogen bonds, but in general, enamines with a carbon−carbon double bond substituted by the hydroxyl group (**19a**−**d**), are more stable than those with allylic hydroxyl groups (**19e**−**h**). The enol resonance stabilizes the species with the hydroxyl substituted directly on the double bond, even though both amine and hydroxyl groups are attached to the double bond at the same time. For comparison, 1-hydroxypropene is more stable than 3-hydroxypropene (allyl alcohol) by 7.8 kcal/mol by B3LYP/6-31G*.

Transition states for the reactions of the hydroxyacetone enamine, **18**, with acetaldehyde, **20a** and **20b** (Figure 8), involve the *Z*-enamine. These are lower in energy than the transition states, **20c** and **20d**, involving the *E*-enamine, primarily due to the extra hydrogen bonding provided by the OH group of the enamine to the forming alkoxide in transition states **20a**

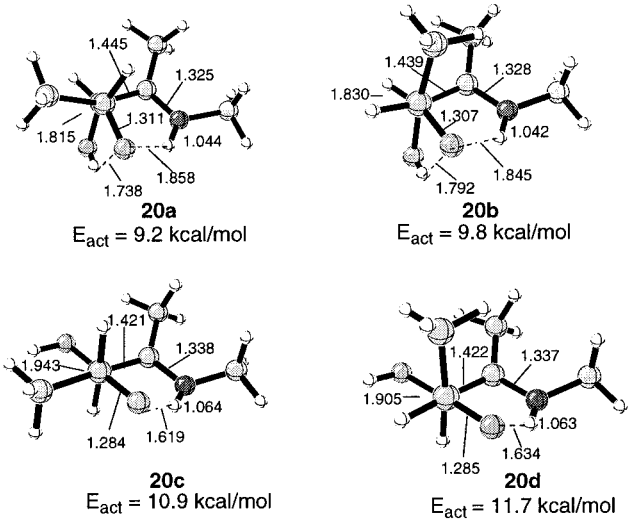

Figure 8. Transition states for the reaction of enamine **18** and acetaldehyde.

Scheme 14. Reaction of Enamine **21** with Acetaldehyde

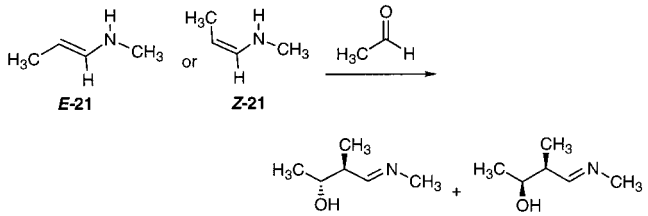

and **20b**. Transition states with axial methyl groups (**20b** and **20d**) are destabilized by 0.6−0.8 kcal/mol.

Diastereoselectivity: Syn/Anti Selectivity in Reactions of Substituted Enamines and Aldehydes. We explored the reactions of the *Z*- and *E*-isomers of substituted enamines with acetaldehyde to explore the syn/anti stereoselectivity of the reaction and to compare it to the well-established preferences found in base-catalyzed aldol processes.[30,31] The reactions of the *E*- and *Z*-isomers of *N*-methylpropenylamine, **21**, with acetaldehyde (Scheme 14) result in four half-chair transition states (Figure 9). (*E*)-**21** is 0.5 kcal/mol more stable than (*Z*)-**21**, and both transition states involving (*E*)-**21** are more stable than those incorporating (*Z*)-**21** by a larger amount. The lowest energy transition state, **22a**, has an axial methyl conformation;

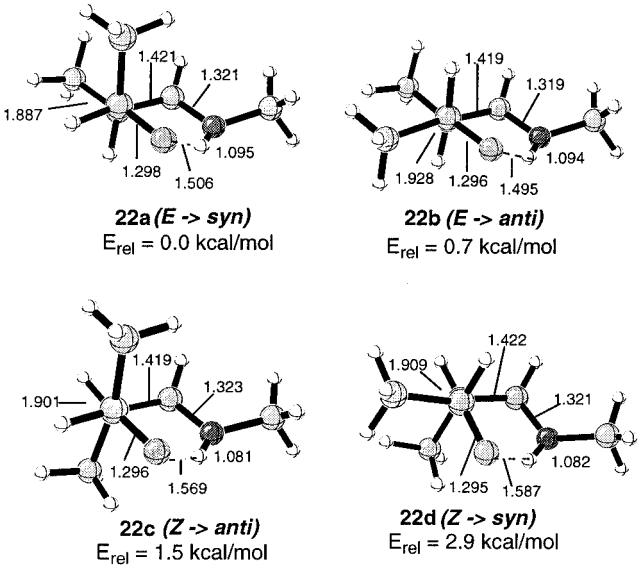

Figure 9. Transition states for the reaction of enamine **21** with acetaldehyde.

Scheme 15. Reaction of 2-Methylamine-2-butene (**23**) with Acetaldehyde

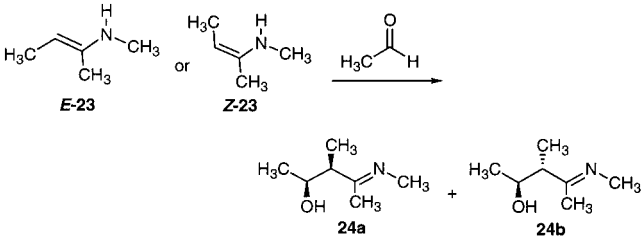

as noted before, the enamine hydrogen is rotated back and does not contribute to steric repulsion. The transition states with equatorial methyl groups, **22b** and **22d**, are destabilized due to gauche interactions with the vicinal methyl groups of the enamine. The *E*-enamine is predicted to favor formation of the syn aldol product by 0.7 kcal/mol, whereas the *Z*-enamine gives the anti, with a 1.5 kcal/mol preference. The transition states for reactions of 2-methylamine-2-butene, **23**, are similar (Scheme 15, Figure 10). (*E*)-**23** favors the syn transition state, **25a**, and (*Z*)-**23** favors the anti, **25c**.

Although the Zimmerman−Traxler transition states provides a rationale of the real *E* → anti and *Z* → syn rule for reactions of aldol reactions involving metal enolates, aldol reactions involving enolates formed from aldehydes give low selectivity in the opposite sense.[30,31] The aldehyde enamines studied here also predict *E* → syn and *Z* → anti preference with low selectivity.

Facial Stereoselectivity with Chiral Aldehydes. Reymond and co-workers reported the stereoselective reaction of acetone and chiral aldehyde **26** catalyzed by primary amine **1**. Aldol products, *syn*-**27**:*anti*-**27**, were obtained in a 1.5:1 ratio (Scheme 16).[9] We explored the stereoselectivity of this reaction using a model system, acetaldehyde enamine, **15**, and chiral aldehyde, **28** (Scheme 17). Two diastereomeric transition states with the equatorial (**30a**) and axial (**30b**) conformations of the pro-S aldehyde were explored (Figure 11). The lowest energy transition state, **30a**, leads to the formation of a product with the same relative stereochemistry of the experimentally observed product, *syn*-**26**. The diastereomeric transition state, **30c**, is 0.3 kcal/mol higher in energy than **30a** and is destabilized due to gauche interactions between the ethyl group of the side chain

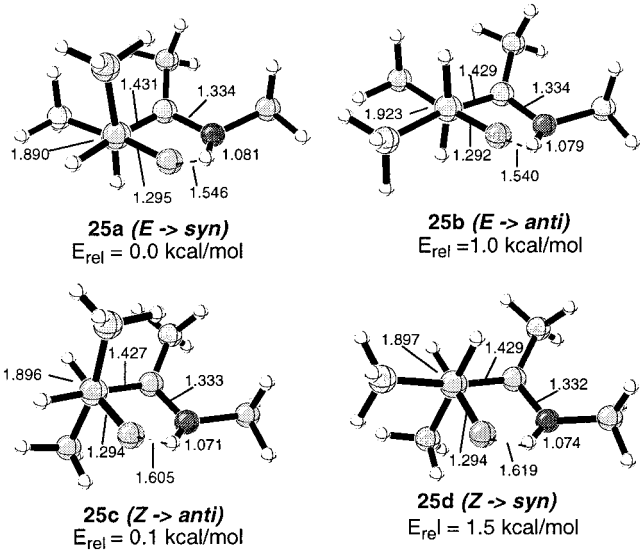

Figure 10. Transition states of the reaction of 2-methylamine-2-butene (**23**) with acetaldehyde.

Scheme 16. Reaction of Acetone with Aldehyde **26** Catalyzed by Primary Amine **1**

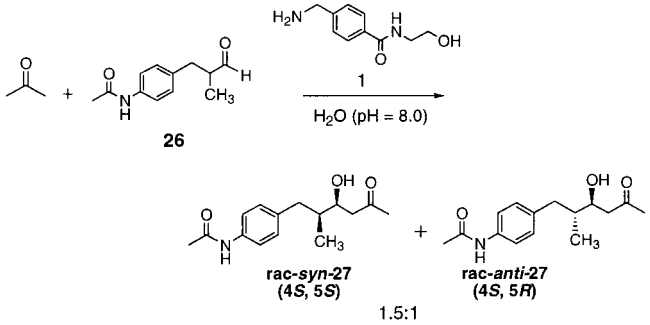

Scheme 17. Products of the Reaction of Enamine **15** with Aldehyde **28**

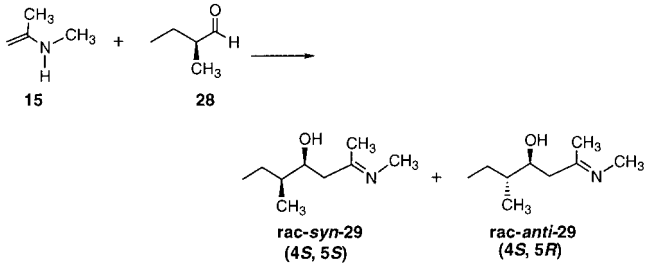

and a hydrogen of the enamine. These interactions are slightly less destabilizing in transition state **30a**, since here the methyl group has gauche interactions with the enamine hydrogen. Transition states **30b** and **30d** are higher energy transition states due to the axial conformation of the moderately bulky side chain. The experiments give a 1.5:1 ratio of stereoisomers *syn*-**27** and *anti*-**27**, and the calculations predict the same distribution of stereoisomers, *syn*-**29** and *anti*-**29**. The reaction follows the normal Felkin−Anh course, with nucleophilic attack anti to the largest group (Et), the medium group inside (Me), and the smallest outside (H).[32]

Intramolecular Aldol Reactions with Primary and Secondary Amines. Intramolecular reactions related to the proline-

(32) (a) Eliel, E. L.; Wilen, S. H.; Mander, L. N *Stereochemistry of Organic Compounds*; John Wiley and Sons: New York, 1994; pp 876−891. (b) Wu, Y.-D.; Houk, K. N. *J. Am. Chem. Soc.* **1987**, *109*, 908−910.

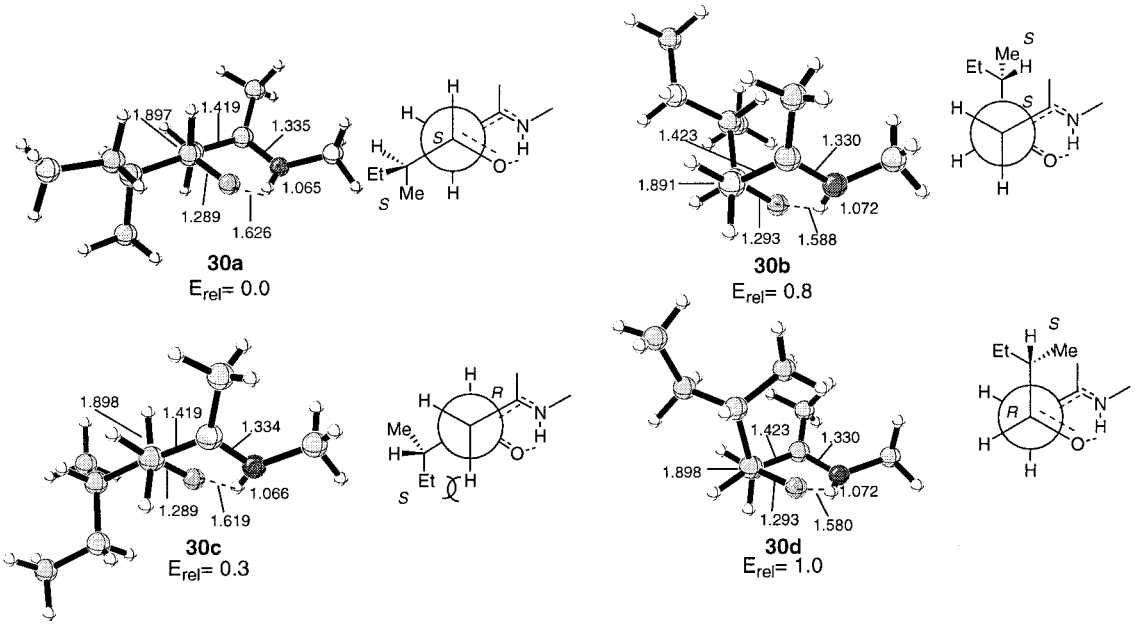

Figure 11. Transition states for the reaction of enamine **15** and aldehyde **(*S*)-26**.

Scheme 18. Intramolecular Reactions of Enamines from Primary and Secondary Amines

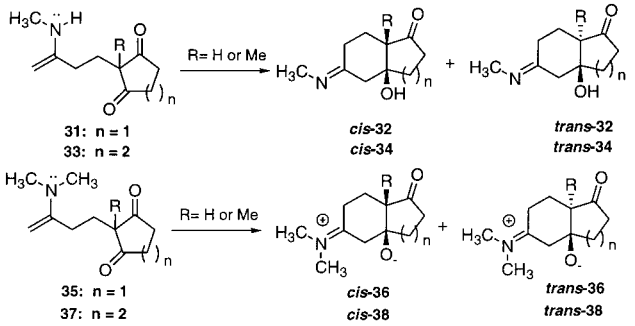

catalyzed Hajos−Parrish−Wiechert reactions shown in Scheme 5 were explored. The formations of both hydrindanones and decalones were explored with primary and secondary amines (Scheme 18). Cis or trans products are possible, and the stereoselectivity is determined by whether nucleophilic attack occurs syn or anti to R, or to the tether that includes the diketone ring.

As in the previous examples, the reaction is expected to occur by a half-chair transition state, involving the enamine N−C═C and the carbonyl C═O, as well as the NH with the primary amine. These groups are already connected by a polymethylene tether, and the enamine, tether, and carbonyl carbon can form either a six-membered chair or boat conformation.

With the *N*-methylenamine **31** (R = H), the cis chair (**39a**), trans chair (**39b**), and cis boat (**39c**) transition states were located (Scheme 18, Figure 12). They are relatively late transition states, with forming C−C bond lengths of 1.74−1.79 Å and C−N bond lengths of 1.33 Å. The reaction via the cis chair transition state, **39a**, has an energy barrier that is 5 kcal/mol below that of the cis boat transition state, **39**. The trans chair, **39b**, has an energy barrier that is 6 kcal/mol higher in energy than that of the cis chair, **39a**.

Several elements contribute to why **39a** is so much more stable than **39b**. In transition state **39a**, the nucleophilic attack occurs syn to the axial group of the five-membered ring, while in **39b**, the attack is anti; the favored attack leads to the formation of the cis product.

The cis-fused transition state **39a** allows for the ideal half-chair arrangement of the five heavy atoms involved in bond formation. This geometry resembles the ideal half-chair transition states for the intermolecular reactions discussed earlier, with a shorter hydrogen bond (1.59 Å) between the NH and forming alkoxide in transition state **39a**; the trans-fused transition state, **39b**, has a distorted arrangement with a much longer H-bond distance (1.81 Å).

Cis hydrindanones have favorable electrostatic interactions between the carbonyl group of the five-membered ring and the electron-rich enamine π bond. This results in a smaller dipole (3.0 D) in **39a** than in **39b** (5.0 D). These effects are also observed and exaggerated in transition states **39d** and **39e**, where R = Me. Here, the axial methyl group further destabilized transition state **39e**, and this is now 11 kcal/mol higher in energy than **39d**. Related to the preference for **39a** is the inherent stability of cis hydrindanone systems relative to trans forms.[33] While trans hydrindanes are more stable than cis hydrindanes, this preference is reversed when the methylene group is replaced by a carbonyl group; *cis*-1-hydrindanone is more stable than the trans form.[33]

Similar transition states were explored for dimethylamine-promoted intramolecular aldol reactions of enamine **35** to form *cis*-**36** and *trans*-**36** (Scheme 18). Because of the absence of intramolecular hydrogen bonding to the developing alkoxide, transition states *cis*-**36** and *trans*-**36** have much larger activation energies. The cis- and trans-fused transition states are now nearly equal in energy (Figure 13).

Transition states were located for the analogous reactions leading to the decalin system (Scheme 18). When R = H, the cis- and trans-fused chair transition states are equal in energy (Table 1). The forming C−C bond lengths are 1.74−1.75 Å, and the C−N bond lengths are both 1.33 Å. Both the cis- and trans-fused chair transition states stabilize the developing charges by hydrogen bonding (1.63 Å in cis and 1.67 Å in trans) through the usual half-chair arrangement. When R = Me, the trans

(33) (a) Eliel, E. L.; Wilen, S. H.; Mander, L. N. *Stereochemistry of Organic Compounds*; John Wiley and Sons: New York, 1994; pp 773−777. (b) House, H. O.; Ramusson, G. H. *J. Org. Chem.* **1963**, *28*, 31−34. (c) Allinger, N. L.; Tribble, M. T. *Tetrahedron* **1972**, *28*, 1191−1201. (d) Sellers, P. *Acta Chem. Scand.* **1970**, *24*, 2453−2458.

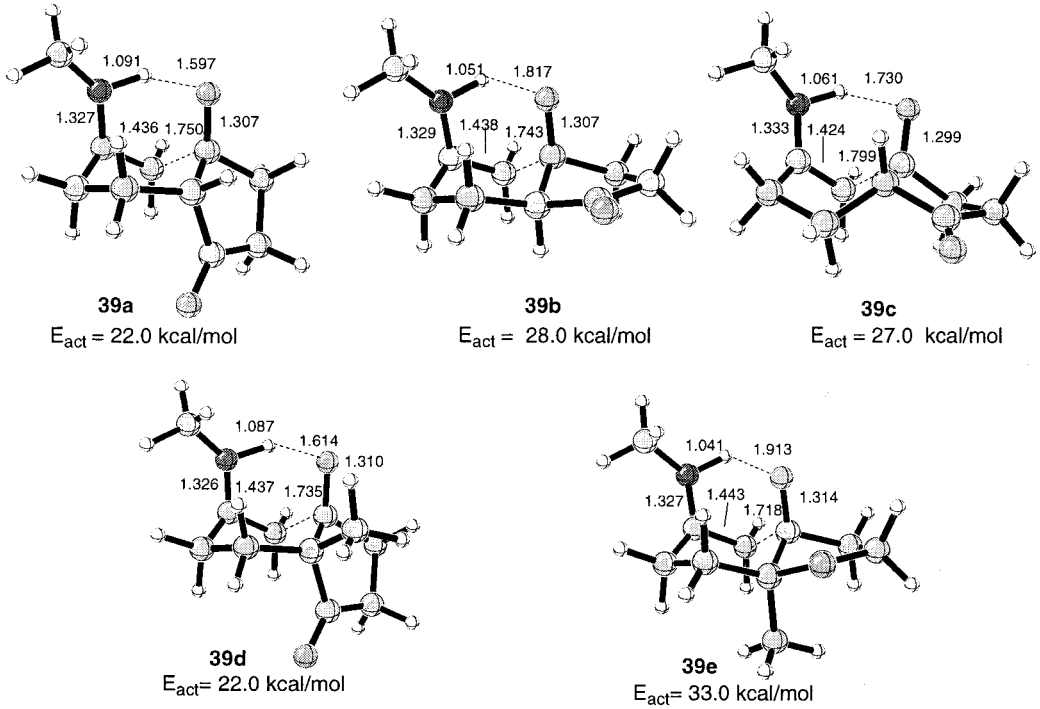

Figure 12. Transition states for intramolecular cyclizations of enamine **31** when R = H (**39a**−**c**) and R = Me (**39d** and **39e**).

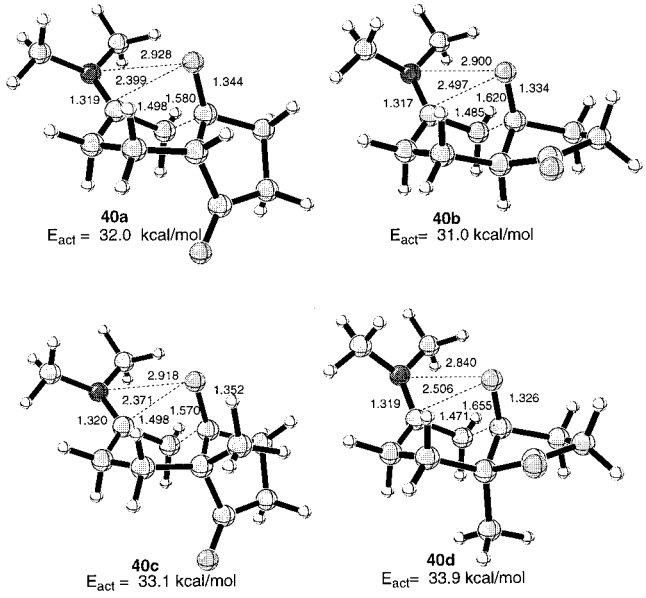

Figure 13. Transition states for intramolecular cyclizations of enamine **33** when R = H (**40a** and **40b**) and R = Me (**40c** and **40d**).

Table 1. B3LYP/6-31G* Relative Energies (kcal/mol) for Transition States of Primary Amine (**33**) and Secondary (**37**) Enamine-Mediated Intramolecular Cyclizations Leading to Decalone-β-ketol Products

reaction	R = H	R = Me
33 → *cis*-**34**	0.0	0.0
33 → *trans*-**34**	0.1	4.0
37 → *cis*-**38**	0.0	0.0
37 → *trans*-**38**	0.8	1.7

transition state becomes 4.0 kcal/mol higher in energy than the cis transition state due to the axial methyl group (Table 1).

The secondary enamine-mediated reactions leading to decalones were also studied (Scheme 18, Table 1). When R = H, the cis-fused transition state is preferred over the trans-fused transition state by only 0.8 kcal/mol. When R = Me, the trans-fused transition state is destabilized due to the axial methyl group, and the cis-fused transition state becomes favored.

In general, we find that there is preferential formation of the cis isomer of bicyclic systems when R = Me. This is in agreement with experimental results where the formation of these *cis*-decalone-β-ketol (**4**) and *cis*-hydrindanone-β-ketol (**6**) ring systems have been reported.[4,5,8−10]

Conclusions

The analysis of the transition states of primary enamine-mediated aldol reactions reveals that the hydrogen bonding in the transition state is essential for stabilization of the developing charges. Hydrogen bonding lowers the activation energies of these reactions. Secondary enamine-mediated aldol reactions have high activation energies and form oxetanes in the absence of a proton source.

The transition states for enamine-mediated intermolecular aldol reactions are half-chair six-membered rings, with the five heavy atoms in an envelope arrangement. There is a gauche arrangement of the enamine and carbonyl double bonds and staggering about the forming bond.

The computed transition states provide models for understanding the stereoselectivities of these reactions. The aldehyde enamines, similar to the metal enolates of aldehydes, are predicted to give *E* → syn and *Z* → anti preference with low selectivity. Ketone enamines are likely to give the *E* → anti and *Z* → syn preference, similar to metal enolates of ketones. The facial selectivity of the enamines was also studied; the Felkin−Anh approach where nucleophilic attack occurs anti to the largest group is favored. For the intramolecular reactions to give hydrinanone and decalones, there is a preference for the formation of the cis-fused rings, in agreement with experiment.[4,5,9−11] Studies of proline- and antibody-catalyzed reactions are in progress.

Acknowledgment. We are grateful to Professors Richard Lerner, Ehud Keinan, Carlos Barbas III, and Benjamin List for

helpful discussions and suggestions. We thank the National Institute of General Medical Sciences, National Institutes of Health (GM 36700), for financial support of this research, and the National Computational Science Alliance (MCA93S015N), the National Science Foundation (CHE-9610080), and UCLA Academic Technology Services for computer resources.

Supporting Information Available: Cartesian coordinates of all reported structures, as well as the total electronic and zero-point vibrational energies (PDF). This material is available free of charge via the Internet at http://pubs.acs.org.

JA011403H